

Impact of the 1997/98 ENSO on upper ocean characteristics in Marguerite Bay, western Antarctic Peninsula

Michael P. Meredith

Proudman Oceanographic Laboratory, Bidston Observatory, Prenton, UK

Ian A. Renfrew,¹ Andrew Clarke, and John C. King

British Antarctic Survey, Cambridge, UK

Mark A. Brandon

Department of Earth Sciences, Open University, Milton Keynes, UK

Received 15 January 2003; revised 22 June 2004; accepted 13 July 2004; published 24 September 2004.

[1] A year-round sequence of hydrographic casts is used to trace the evolution of the upper ocean waters in Marguerite Bay, western Antarctic Peninsula (wAP), between 1998 and 2002. Winter 1998 was anomalous, showing an unusually deep mixed layer that became progressively more saline until spring, reaching salinities as high as 34.0. The remnant of this mixed layer (the Winter Water, WW) was the deepest and most saline observed. Atmospheric and cryospheric conditions were anomalous during winter 1998 at both local and regional scales. Locally, we observed low sea ice concentrations, high air temperatures, and a high frequency of northerly winds. These are the local manifestations of the strong ENSO event of 1997/1998 that was then rapidly weakening. At the regional scale, this ENSO produced significant anomalies in the sea ice distribution throughout the Amundsen-Bellingshausen Sea area, and a large-scale low-pressure anomaly over the southeast Pacific was seen to be responsible for the warm, northerly winds. We use a coupled mixed-layer/ice production model to investigate the ENSO-driven forcings for the anomalous ocean conditions observed in winter 1998. This reveals that ice production is the main control on upper ocean stratification, and that the deep, saline mixed layer in 1998 was forced by anomalous sea ice conditions on spatial scales larger than purely local. We conclude that the near-coastal hydrography along the Peninsula shows a profound response to ENSO, with atmospheric and cryospheric forcings both implicated. *INDEX TERMS*: 4207 Oceanography: General: Arctic and Antarctic oceanography; 4522 Oceanography: Physical: El Niño; 4536 Oceanography: Physical: Hydrography; 4540 Oceanography: Physical: Ice mechanics and air/sea/ice exchange processes; *KEYWORDS*: Antarctic Peninsula, ENSO

Citation: Meredith, M. P., I. A. Renfrew, A. Clarke, J. C. King, and M. A. Brandon (2004), Impact of the 1997/98 ENSO on upper ocean characteristics in Marguerite Bay, western Antarctic Peninsula, *J. Geophys. Res.*, 109, C09013, doi:10.1029/2003JC001784.

1. Introduction

[2] The climate variability of Antarctica and the Southern Ocean has been of increasing interest in recent years, spurred by descriptions of coupled oscillatory modes of surface temperature, sea ice, sea level pressure, meridional wind, and sea level [e.g., *Murphy et al.*, 1995; *Jacobs and Mitchell*, 1996; *White and Peterson*, 1996]. For the region west of the Antarctic Peninsula (Figure 1), *Venegas et al.* [2001] observed that interannual oscillations with a period of around 3–6 years dominated the winter atmospheric and ice variability in the Ross, Amundsen, and Bellingshausen Seas for

the period 1979–1998. They showed that anomalies in sea ice concentration and sea ice drift propagated eastward in the winter ice pack coupled to sea level pressure anomalies, though they did not address the possible effects of this on upper ocean characteristics. *Venegas and Drinkwater* [2001] presented an analogous mode in the Weddell Sea (east of the Antarctic Peninsula; Figure 1).

[3] Several studies [e.g., *Peterson and White*, 1998] have linked Antarctic and Southern Ocean climate variability with climate variability at lower latitudes, specifically the Southern Oscillation. This phenomenon is the characteristic switching of the surface pressure anomaly between the Indian Ocean–Australian region and the southeastern tropical Pacific between high and low states, and is quantified by the Southern Oscillation Index (SOI). El Niño (or El Niño–Southern Oscillation (ENSO)) events are associated with strong negative phases of the SOI.

¹Now at School of Environmental Sciences, University of East Anglia, Norwich, UK.

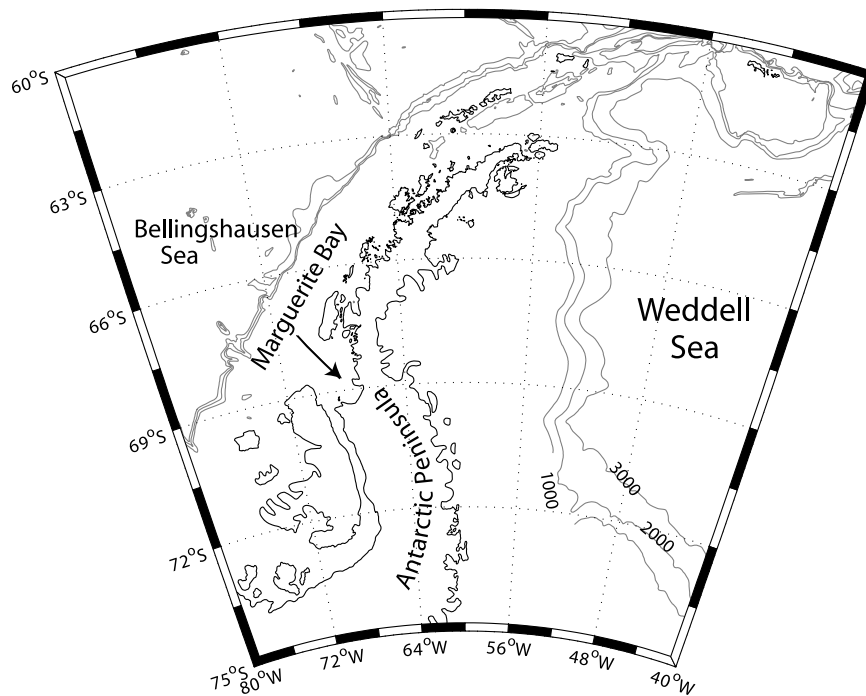


Figure 1. Location of Marguerite Bay on the western Antarctic Peninsula. The 1000-, 2000-, and 3000-m bathymetric contours are plotted. Finer-scale bathymetry is shown in Figure 2.

Cullather et al. [1996] demonstrated a reasonably robust connection between atmospheric circulation in the region of West Antarctica and ENSO.

[4] *Hanna* [2001] reported an anomalous peak in the area of winter sea ice in 1998 for the Ross Sea, the western Pacific Ocean, and the Southern Hemisphere as a whole, and postulated a link with that year's exceptionally strong ENSO event [*Slingo*, 1998] through atmospheric teleconnections. More recently, *Meredith et al.* [2003] showed anomalous sea ice conditions at the Antarctic Peninsula in winter 1998, and demonstrated that the increased sea ice production associated with these conditions had been responsible for an enhancement of downslope convection observed close to the tip of the Peninsula. *Renfrew et al.* [2002a] examined coastal polynya activity in the southern Weddell Sea during 1992 to 1998, and found an anomalously large area of open water during the spring and summer of 1997/1998. This had a profound impact on the surface energy budget, thus modifying the regional ocean energy budget. Both *Ackley et al.* [2001] and *Renfrew et al.* [2002a] suggested that this anomalous sea ice pattern may have been linked to the 1997/1998 ENSO event. *Meredith et al.* [2004] examined a time series of hydrographic data from around the island of South Georgia, in the Atlantic sector of the Southern Ocean, and found that conditions in early 1998 were clearly anomalous due to the influence of ENSO, with both advective effects and strong air-sea fluxes being important.

[5] *Kwok and Comiso* [2002] examined SOI-related anomalies in the Antarctic climate and sea ice cover for the period 1982–1998, and noted that the strongest correlations with the Southern Oscillation were found in the Bellingshausen, Amundsen, and Ross Sea regions. At the peak of ENSO warm events (negative SOI), the climatological low pressure center in the Amundsen-

Bellingshausen Sea weakens, leading to a reduction in the northerly component of the surface winds in the West Antarctic Peninsula sector. This, in turn, promotes lower surface temperatures and anomalously extensive sea ice. *Harangozo* [2000] showed that the opposite response occurs when tropical Pacific sea surface temperatures are rapidly cooling after a warm ENSO event. In this case the Amundsen-Bellingshausen low deepens, northerly flow in the west Antarctic Peninsula region strengthens, surface temperatures increase, and sea ice cover is anomalously low. Such were the conditions prevailing during the austral winter of 1998, when the strong ENSO warm event of 1997/1998 was rapidly decaying.

[6] The oceans close to Antarctica present extreme problems for studies of seasonal and interannual variability. While sea ice concentration can be mapped at large scales (but low resolution) using passive microwave data from satellites, remotely sensed measurements of sea surface height (and hence current speed variability), sea surface temperature (SST), and so on are often rendered impossible by the very presence of the ice. In addition, cloud cover often obscures the ocean surface close to the Antarctic continent, affecting remote sensing at infrared and visible wavelengths. In situ studies have the potential to circumvent these problems, as well as yielding information on ocean structure below the surface, but such studies tend to be concentrated in the austral summer when access by ship is easiest.

[7] Despite the difficulties, these regions are highly important, as they are subject to some of the most intense longer-term climatic changes occurring in the world. For example, the western Antarctic Peninsula wAP (Figure 1) has undergone the most dramatic warming of any region in the Southern Hemisphere [*King*, 1994; *King and Harangozo*, 1998], with mean annual temperatures increasing by more than 2.5°C over the last 50 years.

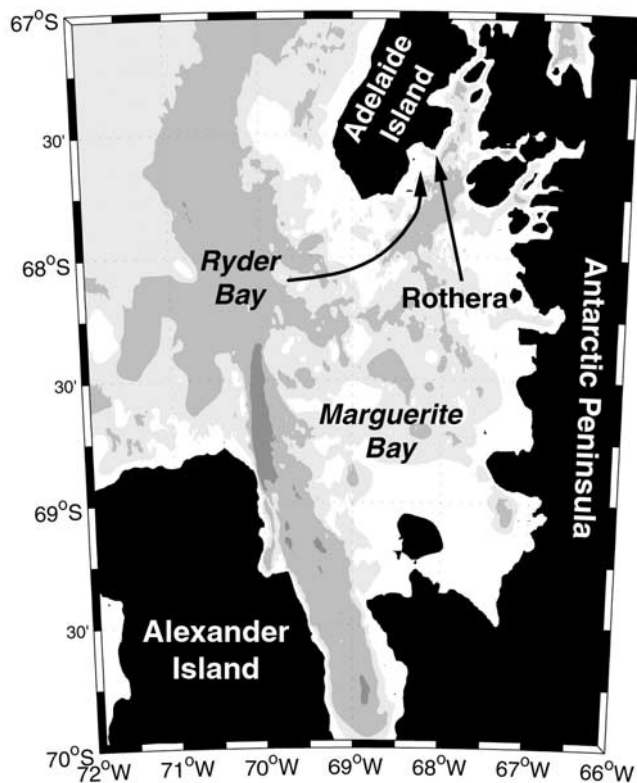


Figure 2. Location of the British Antarctic Survey research station at Rothera, Adelaide Island, and the Rothera Time Series (RaTS) sampling site in Ryder Bay. Bathymetric data are from the recently compiled Southern Ocean Global Ecosystems Dynamics (GLOBEC) data set; contour intervals are <1500 m (darkest), 1000 m, 500 m and >250 m (white).

Associated with this has been a progressive collapse of the northern Peninsula ice shelves. The impact of such changes on the marine environment is virtually unknown, a situation that is exacerbated by the warming occurring most strongly in the austral winter, the period when in situ data collection is most challenging.

[8] In recent years, we have built up a year-round series of upper ocean hydrographic casts from Marguerite Bay on the wAP (Figure 1). This time series, which commenced in 1998, is extremely valuable since it gives almost unprecedented temporal coverage and resolution. The attendant drawback is, of course, the lack of spatial coverage. However, even without direct information on variability in local ocean circulation and spatial changes in properties, there is much that a systematic, prolonged time series can tell us about the oceans' response and role in climate variability. We use this time series here to examine the characteristics of seasonal and interannual changes in the Antarctic physical environment, and, in particular, address the nature and causes of observed anomalous ocean properties during the austral winter of 1998.

2. Background

[9] Marguerite Bay is enclosed by Adelaide Island to the north, Alexander Island to the south, and the Antarctic

Peninsula to the east (Figure 2). A deep trench between Adelaide and Alexander Islands (the Marguerite Trough, down to 750 m) connects the center of Marguerite Bay with the shelf edge to the northwest. The water mass structure over the wAP continental shelf is relatively simple, and has been described in detail previously [e.g., Hofmann *et al.*, 1996; Smith *et al.*, 1999]. The source water is Upper Circumpolar Deep Water (UCDW), a warm, saline water mass of the Antarctic Circumpolar Current (ACC) that is also characterized by a relative minimum in dissolved oxygen and maxima in dissolved nutrients [Callahan, 1972; Sievers and Nowlin, 1984]. Above this lies the Antarctic Surface Water (AASW), commonly considered to be the water at the surface that is warmed by insolation and freshened by ice melt during summer. Typical AASW properties are warmer than 0°C and/or fresher than around 33.5 within northern Marguerite Bay. During winter, a thick layer of colder, more saline water occupies the upper layers of the water column. The deep remnant of this winter mixed layer that persists through the austral summer is generally marked by a subsurface temperature minimum; this is termed Winter Water (WW [Mosby, 1934]). The characteristics of Marguerite Bay waters are similar to those of the general wAP shelf, as will be seen below.

[10] The UCDW that penetrates onto the continental shelf of the wAP is often modified, becoming cooled and freshened. Klinck [1998] postulated that deep channels across the shelf and shelf break, such as the Marguerite Trough, are likely to be important sites for the transfer of UCDW onto the shelf. Meanders of the ACC may induce variability in this transfer, and in the subsequent properties of the UCDW on the shelf [Klinck, 1998]. Smith *et al.* [1999] showed that the modification of the shelf UCDW could be explained by a balance between across-shelf diffusion of heat and salt from offshore UCDW and vertical diffusion of heat and salt across the permanent pycnocline into the WW layer; it should be noted, however, that this does not preclude variability in advective transfer of UCDW onto the shelf. Klinck [1998] examined heat and salt changes on the wAP between 1993 and 1994, and found that the changes above the pycnocline followed a seasonal pattern of cooling and increasing salt from summer to winter, and warming and freshening from winter to summer. He found that the year-to-year difference was small compared with the seasonal change, and that while there were changes below the pycnocline, they showed no obvious seasonality.

[11] To investigate the key processes that determine sea ice and upper ocean properties in the wAP region, Smith and Klinck [2002] constructed and ran a vertical, time-dependent sea ice and mixed layer model. They found that diffusive-convective instability is important for upward heat flux across the pycnocline, and that direct melting of ice by solar heating is negligible, with warming of the water (which then melts the sea ice) being the dominant mechanism for this. They also argued for the importance of UCDW intrusions onto the shelf in both the heat and salt budgets of the area.

[12] There have been some significant recent advances in our understanding of Marguerite Bay and the wAP from work undertaken within the Palmer Long Term Ecological

Research (LTER) Program [Smith *et al.*, 2003] and as part of the Southern Ocean contribution to the Global Ecosystem Dynamics (GLOBEC) programme. Klinck *et al.* [2004] observed, using hydrographic data, the presence of a coastal current that flowed southward along Adelaide Island into Marguerite Bay, and, after leaving the bay, subsequently southward along Alexander Island (Figure 2). They suggested that this current may be the result of seasonal coastal buoyancy forcing, and observed that it was present in autumn and winter. Beardsley *et al.* [2004] used data from passive drogued drifters to investigate the coastal current, and derived speeds of around 10 cm s^{-1} , rising up to 20 cm s^{-1} during periods of high winds. They observed that the location and orientation of the coastal current within Marguerite Bay depends on the sea ice present at the time. Klinck *et al.* [2004] noted intrusions of UCDW onto the continental shelf and into Marguerite Bay via, in particular, the Marguerite Trough, and suggested that such intrusions could be a frequent occurrence (4 to 6 per year). This was investigated in the model study of Dinniman and Klinck [2004], who found that the penetration of UCDW onto the shelf depended on momentum advection and the curvature of the shelf break, with the general shelf circulation then tending to draw UCDW into the interior.

3. Methods

3.1. Oceanographic Observations

[13] As part of the Rothera Time Series (RaTS) project, a Chelsea Instruments Aquapack Conductivity-Temperature-Depth (CTD) instrument was used to profile the upper ocean characteristics at a site in northern Marguerite Bay between 1998 and 2002. The sampling site was at Ryder Bay, close to the BAS research station at Rothera on Adelaide Island (Figure 2). The instrument package was lowered and raised using a hand-cranked winch, with casts limited to a maximum depth of 200 m by the pressure rating of the instrument (water depth at the sampling site is approximately 400 m). The equipment was operated in self-recording mode, with data downloaded immediately afterwards at the research station. Casts were conducted from an inflatable boat during the ice-free months of the austral summer, and through a hole cut in the sea ice during the austral winter. In addition to the CTD casts, discrete water samples were taken from 15 m depth using a Niskin bottle closed with a brass messenger. Direct measurements of size-fractionated chlorophyll and macronutrient concentrations were made from the discrete samples; these will be reported elsewhere.

[14] Precision of the CTD data was maintained by performing concurrent casts with SeaBird 911plus CTDs during the regular visits of RRS *James Clark Ross* and RV *Laurence M. Gould* to Rothera. The SeaBird salinity data were themselves calibrated using discrete samples measured on a Guildline Autosol 8400B salinometer, standardized with IAPSO P-series standard seawater. Offsets to the Aquapack salinity data were applied to reconcile them with the calibrated SeaBird data.

[15] Densities were calculated using the *U.N. Educational, Scientific, and Cultural Organization* [1983] algorithm. We also calculate the Potential Energy Anomaly

(PEA [Simpson, 1981]) to consider the effects of vertical stratification,

$$\text{PEA} = \frac{1}{h} \int_{-h}^0 (\bar{\rho} - \rho) g z \, dz \quad (1)$$

$$\bar{\rho} = \frac{1}{h} \int_{-h}^0 \rho \, dz,$$

where z is the vertical coordinate, h is the maximum depth, ρ is the density, and g is acceleration due to gravity.

[16] Sampling frequency was approximately weekly when conditions allowed. There were two extended periods during which no data could be collected, namely, August to December in both 2000 and 2001. The first of these was caused by an unusually extended period of unfavorable ice conditions (too heavy for boat operations, and unsafe for sledge operations). The second of these was the result of the loss of the laboratory in a fire; it was not possible to restart observations until replacement equipment arrived with the relief of Rothera Research Station the following December.

3.2. Meteorological and Sea Ice Observations

[17] Direct observations of sea ice, both in terms of ice concentration and ice type, were routinely made for Ryder Bay on an approximately weekly basis. Meteorological observations of mean sea level pressure, 10-m winds, 2-m air temperature, 2-m relative humidity, and cloud fraction are available from the 3-hourly synoptic observations at Rothera. Over the study period, less than 1% of the meteorological data were missing or “bad,” with these gaps generally interpolated across. However, a 2-week period of missing data is replaced by climatological values. Precipitation is not routinely measured at Rothera due to the practical difficulties in distinguishing between falling and blowing snow; hence precipitation values used here are extracted from the ECMWF ERA-40 reanalysis and operational analyses for the model grid point nearest to Ryder Bay. Monthly mean air temperatures measured at Rothera agree closely with those measured by automatic weather stations deployed in Marguerite Bay as part of Southern Ocean GLOBEC during 2001–2003; this indicates that the Rothera air temperature data is a good proxy for that over the larger Marguerite Bay region.

[18] To calculate a surface energy budget for Ryder Bay, the meteorological data were interpolated onto a 6-hourly time series. The total heat flux from the ocean into the atmosphere, Q_{tot} , can be written as $Q_{\text{tot}} = Q_s + Q_l + Q_r$, where Q_s is the sensible heat flux, Q_l is the latent heat flux, and Q_r is the net radiative heat flux. The surface fluxes are calculated as detailed by Renfrew *et al.* [2002a]. The turbulent heat fluxes over open water at freezing point are calculated using a stability-dependent algorithm based on that of Smith [1988] and DeCosmo *et al.* [1996]. This algorithm is discussed in more detail and validated against comparable air-sea conditions by Renfrew *et al.* [2002b]. The long wave and short wave radiative fluxes are calculated from well-established empirical formulae, which use SST, air temperature, humidity, and cloud cover as

input data. These formulae have been shown to be sufficiently accurate for sea-ice modeling purposes when accurate cloud observations are available such as at Rothera.

3.3. Ice Production Model

[19] Following *Renfrew et al.* [2002a], a time series of ice production per unit area is calculated. This is a 1-D model calculation for Ryder Bay and as such, does not account for any advective effects. In short, the total surface heat flux, $Q_{\text{tot}}(t)$, is weighted with the directly observed open water fraction to calculate the oceanic cooling, and thus the ice production from $Q_{\text{tot}} = \rho_i L_f F$, where ρ_i is the density of ice, L_f is the latent heat of fusion, and F is the ice production rate. We make the assumption that ice is only produced when (1) $Q_{\text{tot}} > 0$, that is, heat flux is from the ocean into the atmosphere, and (2) we are within the freezing season. Here, the freezing season is defined as 1 May to 1 November each year, and it is assumed that outside of this period, surface heat loss will lead to a cooling of the ocean rather than ice production. The dates were based on the seasonal pattern of local surface temperatures (Figure 3 in section 4). Monthly sea surface temperature values in the ice production model were also prescribed based on observations. Ice thickness observations are not made routinely, but in some years, up to a dozen are available. It is clear from these that the ice is generally “thin” (less than 0.3 m) when the ice fraction is less than about 0.8 and generally “thick” (more than 0.3 m) when the ice fraction is greater than 0.8. This simple relationship is used to account for ice thickness in the heat flux weighting, as detailed by *Renfrew et al.* [2002a].

3.4. Oceanographic Mixed-Layer Model

[20] An oceanographic mixed-layer model, based on the Price-Weller-Pinkel (PWP) model [*Price et al.*, 1986], was constructed and run, using the air-sea fluxes derived from the meteorological data set detailed as above. Each time step, three criteria for vertical stability are applied; these depend on static stability, the bulk Richardson number criterion, and the gradient Richardson number criterion. Following this, vertical advection and vertical turbulent mixing are applied. Vertical diffusivity (K_z) is assigned a value of $10^{-4} \text{ m}^2 \text{ s}^{-1}$; this value was chosen partly since it was observed to give small levels of unrealistic drift of the model. Other values trailed did not alter the level to which the model was able to reproduce the seasonal or interannual variability of the observations, but rather showed long-period changes that the observations do not support. The diffusivity we use is time invariant; clearly, if the actual mixing were variable, this would not be well reproduced; however, in the absence of more information on this, we are unable to adopt a different approach.

[21] Vertical advection is permitted in the model, but horizontal advection and mesoscale variability are not. Wind stress, calculated from the meteorological observations, is applied as a vector to allow shear at the base of the mixed layer to influence the mixing. Unlike the other components of heat flux (which warm or cool solely the surface of the model ocean), the incoming shortwave radiative heat flux is allowed to penetrate downward a distance that depends on a double exponential function

determined according to the Jerlov classification of the waters, as given by *Paulson and Simpson* [1977].

[22] The PWP model was linked to the sea ice production model (described above) in a one-dimensional, unidirectional sense, with sea ice formation (or melt) acting to inject brine (or cold, low-salinity water) into the surface model ocean. Note that the surface heat fluxes were weighted by the total ice cover, while the surface stresses were weighted by the amount of fast ice cover. Latent heats associated with ice formation and melting were included in the heat budget applied. It was recently highlighted that glacial ice melt can be an important source of freshwater for the waters west of the Antarctic Peninsula [*Dierssen et al.*, 2002]; for our mixed layer model, this was estimated using the relationship between air temperature and glacial melt derived by *Braithwaite* [1984]. The model was run with monthly mean (seasonally repeating) values for 5 years before the derived fluxes were applied for the simulation of 1998 to 2002. The initial 5-year period with seasonally repeating forcing was to allow the model to settle into a regular seasonal cycle before applying realistic forcing. No “nudging” was applied to keep the model in line with observations; this is partly accounted for by the flexibility in the choice of value for vertical diffusivity.

4. Results

4.1. Oceanographic Results

[23] The progression of upper layer potential temperature is shown in Figure 3. Strong seasonality is immediately obvious, with the highest AASW temperatures (up to approximately 3°C) generally found during January to March. During April to July, the isotherms move downward as heat is lost to the atmosphere and the mixed layer deepens, intruding on the temperature minimum of the WW. By the end of May, the temperature minimum of the WW has generally been eroded, and is no longer present. During July to October, surface temperatures are close to (and often at) the freezing point for seawater.

[24] In addition to the seasonal variability, there is also a great deal of interannual variability present in the temperature data. Peak AASW temperatures measured in the austral summers varied by as much as 3°C , although sea ice formation and melting limits the range in the austral winter. The depth of the core of the temperature minimum WW layer varied significantly, from around 50 m below the surface in the austral summer of 1998 and 2000 to nearly 150 m in the austral summer of 1999. Years that have complete coverage from the austral winter show some radically different characteristics: In 1998, virtually the whole water column down to 200 m was isothermal between August and October, while in 1999 and 2002, there was much greater stratification.

[25] As would be expected, there are also clear seasonal signals present in the salinity data (Figure 4). The surface layer is typically freshest from around January/February through to around April, following the melt of the previous winter’s sea ice cover and during the period of greatest freshwater input from melting glaciers on the wAP coast. The onset of ice formation around May/June raises surface salinities as a consequence of brine rejection. This seasonal densification of the surface layer is one factor in the deeper

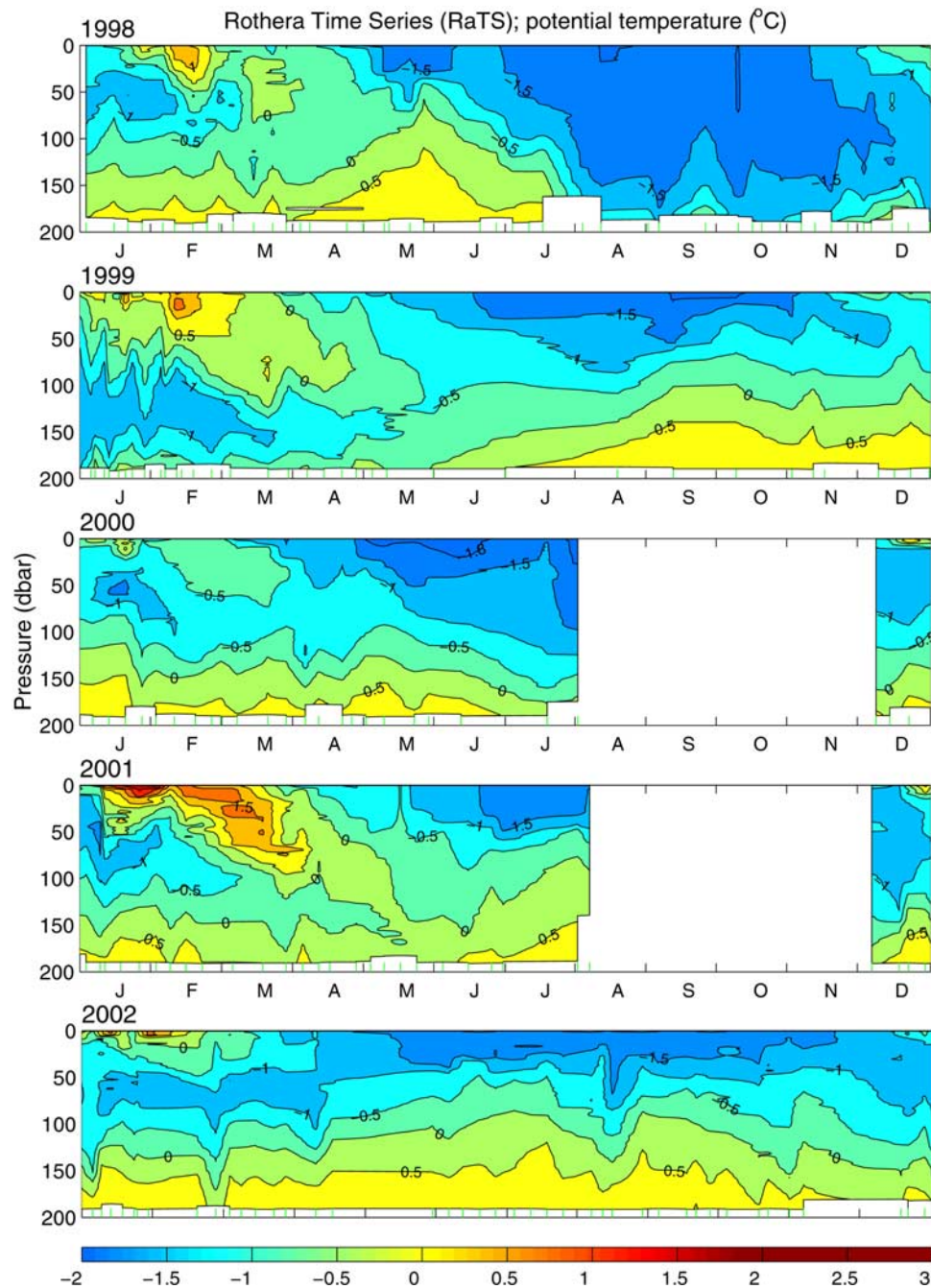


Figure 3. Progression of potential temperature for the upper 200 m at the RaTS sampling site (Ryder Bay, Figure 2). Green tickmarks above the lower horizontal axis denote times of CTD casts. The gap in 2000 was due to unfavorable ice conditions; that in 2001 was due to loss of equipment in a fire.

mixed layers of the austral winter. Also contributing is the higher frequency of atmospheric low-pressure systems in the austral winter, leading to a higher incidence of gale force winds and thereby an enhanced air-sea transfer of momentum and increase in turbulent kinetic energy.

[26] As with the temperature data, the salinity data from the austral winters of 1998, 1999, and 2002 also show some dramatically different characteristics. In winter 1998, the water column was almost entirely isohaline down to 200 m, whereas in winter 1999 and 2002 it was much more stratified. Reasons for this will be elucidated below.

[27] The bottom layer of the data is generally warm and saline, with potential temperatures around 1°C and salinities around 34.4–34.5. In the open ocean, UCDW has potential temperatures over 1.5°C and salinity between 34.6 and 34.7, whereas typical UCDW modified on the WAP shelf has potential temperature in the range 1.0°–1.45°C and salinity over 34.5 [Klinck, 1998]. Thus our casts do not penetrate deep enough to sample the core of the UCDW, but rather sample down into a region of mixing between the top of the UCDW layer and the bottom of the AASW or WW.

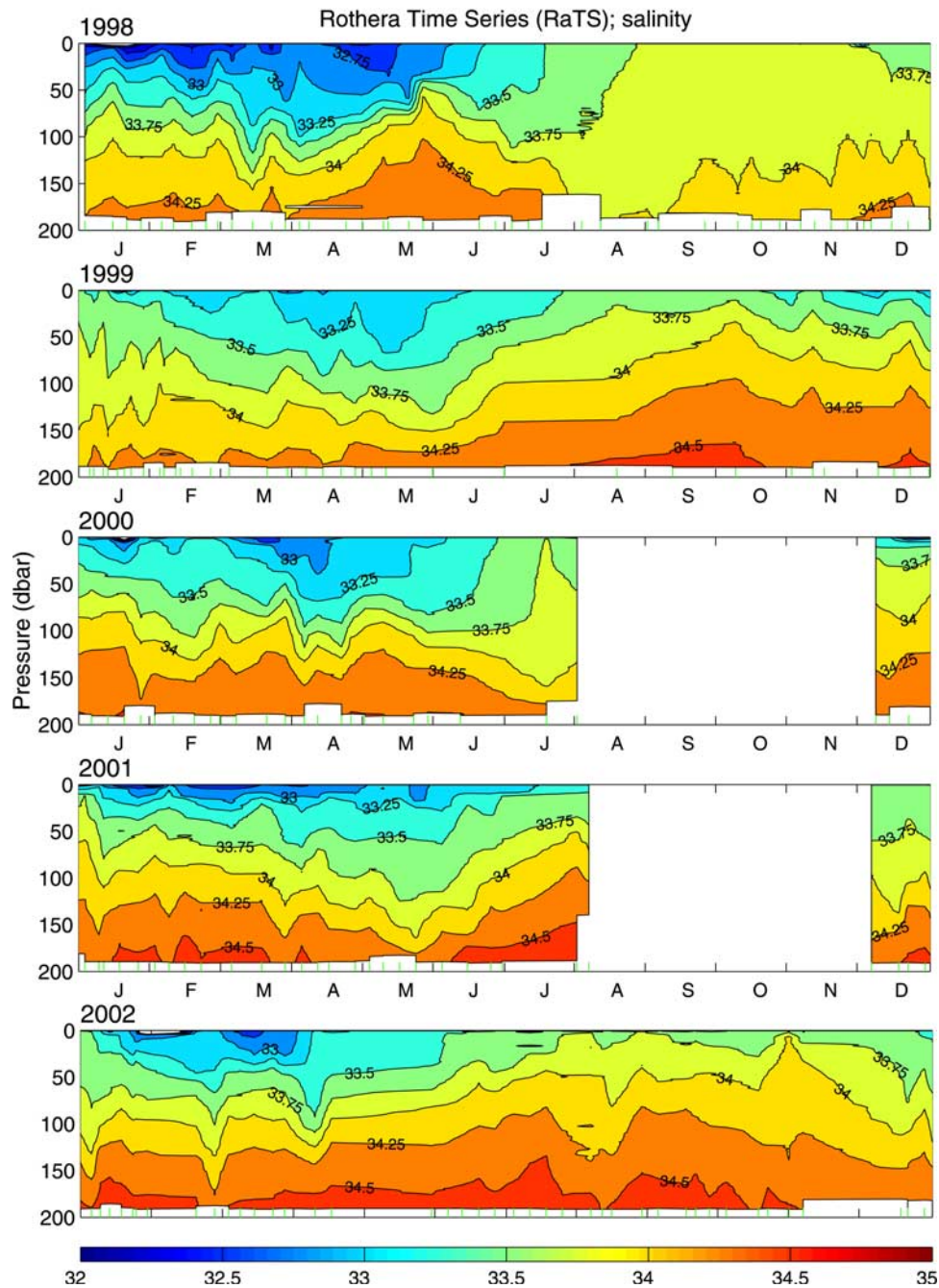


Figure 4. As for Figure 3, but for salinity.

[28] The temporal progression of density (Figure 5) strongly resembles that of salinity, a consequence of salinity dominating the equation of state at low temperatures. Accordingly, the lightest AASW (January/February 1998) coincided with the freshest AASW. Again, the very deep mixed layer in austral winter 1998 is present, and contrasts strongly with the much more stratified layers in winter 1999 and 2002.

[29] Each CTD cast is shown in potential temperature-salinity (θ -S) space in Figure 6 as a function of both month and year. Profiles taken during December to March show a characteristic inflection due to the temperature minimum of the WW at mid-depths. There is a great deal of variability in

the temperature and salinity of the surface ocean for the data from these months. The temperature minimum WW layer shows significant variability in its salinity, ranging from less than 33.5 in January 1998 to approximately 34.0 in January 1999. There is some interannual variability in the very densest UCDW sampled (e.g., January in Figure 6). Although our CTD casts do not penetrate deep enough to discern the true variability at the core of the UCDW on the wAP shelf, projections of the mixing curves shown in Figure 6 would appear not to coincide, suggesting interannual variability in properties of the core UCDW.

[30] The inflection due to the WW persists until around April or May, by which time it is destroyed by cooling of

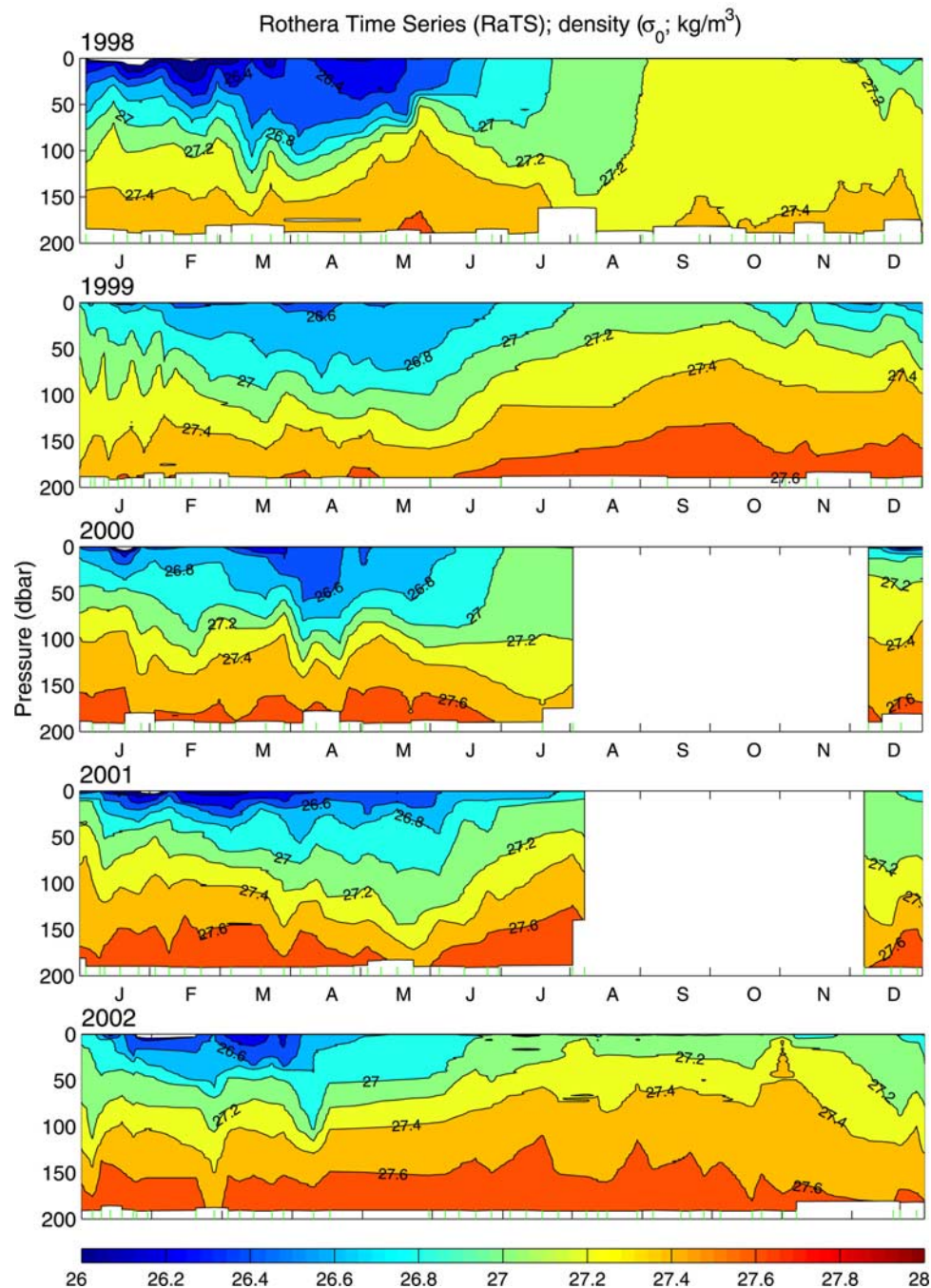


Figure 5. As for Figure 3, but for density anomaly (σ_0).

the surface layer. During the period May to June, surface temperatures reach freezing point and surface salinities begin to increase. Data from around these months show some examples of near-isothermal layers close to the surface; for example, the data from June 2001 show several virtually horizontal lines in θ - S space (Figure 6). There are also indications of such layers in other months and years. (Note that there is some evidence in Figure 6 for such a layer in November 1998, at the start of the seasonal warming). The peculiar appearance of these layers in θ - S space is caused by the difference in depth to which the water is homogeneous in its different physical properties, for

example, typically around 20–40 m for temperature in June, but only around 10–20 m for salinity. The most likely explanation for their formation is that an initial mixed layer, with temperature close to the freezing point, has cold freshwater from ice melt mixed into its upper part. This will significantly decrease the salinity of the upper part of this layer, but its temperature (being at the freezing point already) will not be greatly altered. This leads to temperature being homogeneous to a greater depth than salinity. Since the freshwater has temperature close to zero and very low (or zero) salinity, the temperatures of the oceanic water and freshwater will be very close, but their salinities will be

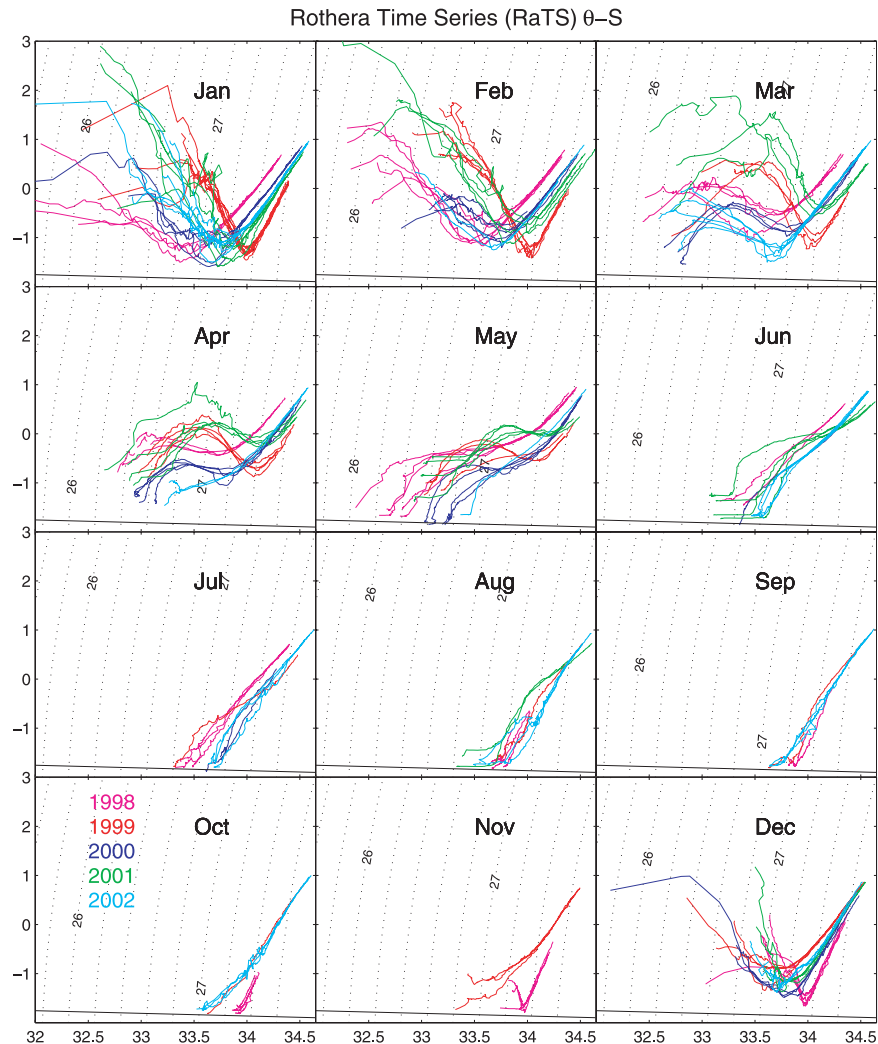


Figure 6. Potential temperature-salinity diagrams for the data collected at the RaTS sampling site (Ryder Bay, Figure 2). Panels are separate months (marked); CTD curves are colored according to the year of data collection: magenta (1998), red (1999), blue (2000), green (2001), and cyan (2002). Contours of density anomaly (σ_0) are plotted (dotted lines) at intervals of 0.2 kg/m^3 . The freezing line (solid line) is plotted across the base of each panel.

very different. Consequently, mixing appears almost horizontal in θ -S space.

[31] These layers appear to occur during some months when the monthly mean air temperature is below zero (e.g., June; Figure 6). However, it is important to note that even in these cold months, there can be days (possibly several) when the temperature rises above the freezing point. Thus, while the mean temperature may be below freezing, these shorter-lived warm periods can lead to brief melting and the formation of these layers. Since the freshwater injected into the surface ocean is not very dense, it will stabilize the upper water column and act to preserve the layer; there is some evidence of them persisting into August (in 2001; Figure 6). The persistence of these layers affects future mixed layer dynamics, since more energy is then required to homogenize the upper water column to a given depth.

[32] For the months July to October, the θ -S curves are close to straight lines between the UCDW and the WW characteristics. The very deep mixed layer observed in the

austral winter of 1998 is apparent as a very short line in θ -S space; for example, October 1998 in Figure 6 shows properties that are almost uniform down to 200 m depth. By comparison, the same month in 1999 shows a much greater range of values, despite the cast being conducted to the same depth. In November, the surface layer begins to warm and freshen as insolation increases and the ice starts to melt. In November 1998 (Figure 6), the temperature minimum of the WW layer has begun again; in 1999 this did not happen until December.

[33] PEA is shown as a function of year and month in Figure 7. PEA represents the energy that would be required to homogenize the layers considered; thus high values for PEA denote a strongly stratified (stable) water column. A fully mixed column would have a PEA of zero. Values for PEA are typically high during January to April, indicating a strongly stratified water column. During August to November 1998, values for PEA were very low (about 10 J m^{-3}), indicating a well-mixed upper water column, i.e., a deep mixed layer. The

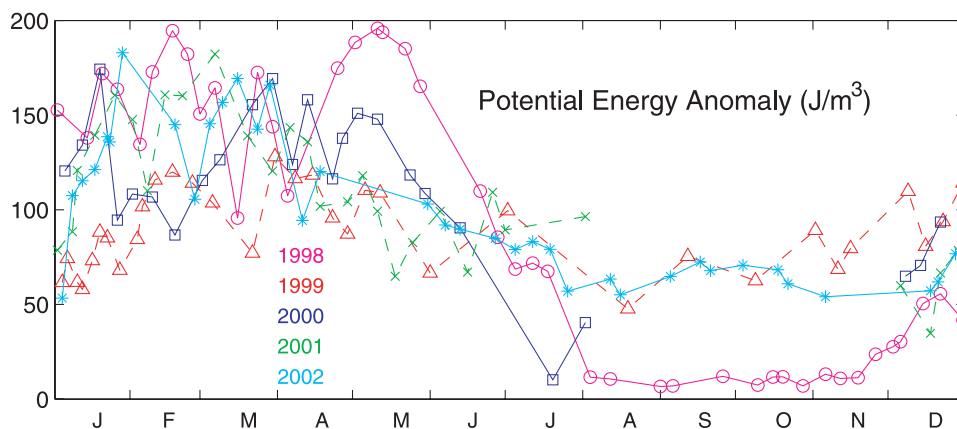


Figure 7. Potential Energy Anomaly (J m^{-3}) for the RaTS data as a function of month and year. Note in particular the very low values during the austral winter of 1998, when the stratification in the upper waters was very low.

values for PEA begin to increase in December 1998, but in general remain low compared with other years. They continue to be relatively low throughout January 1999 and the first half of February 1999 (Figure 7). This is caused by the WW core being deep and saline during the austral summer of 1999 (around 150 m, and 34.0), and the surface layer being saline compared with other years (Figure 4). Consequently, there was a thick upper layer over which there was only a small vertical gradient in salinity, and hence density.

4.2. Meteorological and Sea Ice Observations

[34] To understand the causes of the observed seasonal and interannual variability, we need to examine the physical processes forcing upper ocean structure over the wAP shelf. Figure 8 shows the monthly mean air temperature at Rothera, and Figure 9 shows the observed Ryder Bay sea ice fractions over the study period. The strong seasonality is obvious in both. Air temperatures are highest during the

months December to February (around 0° – 2°C), then decrease thereafter as seasonal cooling progresses. A sharp drop in temperature occurs most years at some point within the period April to August, followed by low winter temperatures through to September (down to around -13°C or colder). A sharp rise in temperature normally occurs during September or October, followed by a warming through to the peak temperatures of December to February. Sea ice fractions show maximum values in the winter, and generally low or no sea ice in the summer. However, the interannual variability in ice concentration is large over the study period; for example, in 2000 the maximum cover is during September to November, while in 2001 it is during June. During 2002, there is near-total ice coverage from April right through to November.

[35] The year 1998 has unusual characteristics in both the sea ice and air temperature data. It has been noted previously [Kwok and Comiso, 2002] that sea ice and air

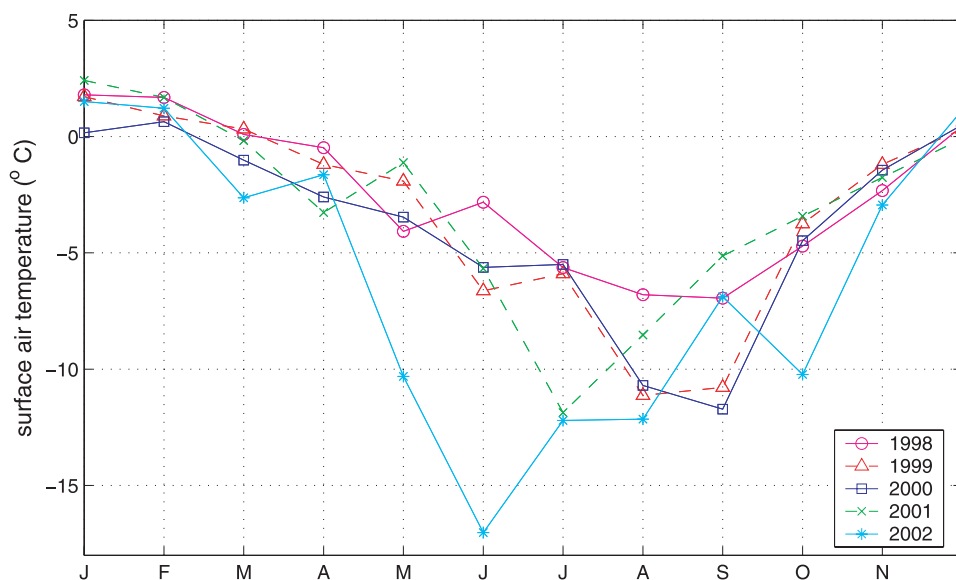


Figure 8. Monthly mean surface air temperature (dry bulb) at Rothera research station as a function of month and year. Note in particular the warmer temperatures during the austral winter of 1998.

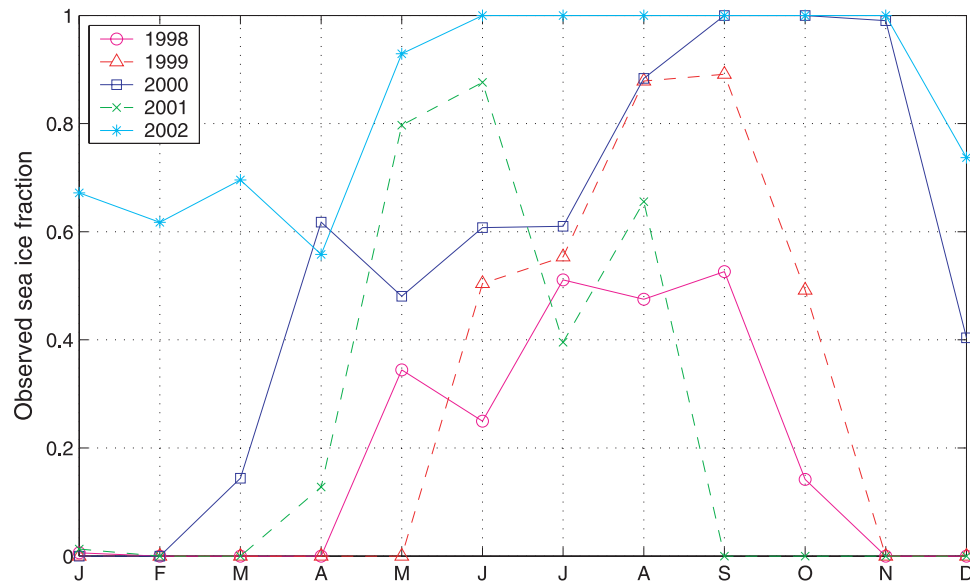


Figure 9. Monthly mean sea ice fraction, independent of ice type, observed at Ryder Bay near Rothera. Note in particular the anomalously low sea ice fraction in the austral winter of 1998.

temperature were anomalous at the regional scale of the wAP in 1998, in response to the 1997/1998 ENSO event that was then decaying; Figures 8 and 9 show the local manifestation of this at the RaTS site. Air temperatures were broadly similar to the other years through the austral summer, but winter temperatures remained persistently high (Figure 8). The minimum monthly mean air temperature in 1998 was around -7°C ; the next lowest during our sequence of measurements was around -12°C . The sea ice fraction remained persistently low throughout the austral winter, with maximum values in September 1998 of around 0.5 (Figure 9), the lowest of any year. It is worth noting that the year of 2002 was also anomalous, but in the opposite sense: Air temperatures dropped dramatically within April and May to reach their coldest values during this 5-year period (around -17°C ; Figure 8), and sea ice fractions were at their highest, with near-total coverage from May right through to November (Figure 9).

[36] The mean sea level pressure anomaly for the austral winter of 1998 is shown in Figure 10. The pattern is representative of those typically seen for a decaying ENSO event [Harangozo, 2000]. Conspicuous is the low-pressure anomaly over the Amundsen-Bellinghousen Sea, linked with more frequent northerly wind episodes on the western side of the Antarctic Peninsula. Warmer temperatures associated with northerly winds can reduce ice production rates over the open ocean and inhibit northward growth of the winter ice cover in the Bellinghousen Sea [Harangozo, 1997]. Anomalously low ice concentrations in the region of the wAP are apparent in Figure 11.

[37] The unusual local meteorological conditions during winter 1998 are further illustrated in Table 1, which details winter season mean meteorological data for Rothera. This shows that along with being the warmest of the years considered here, 1998 was also the windiest. The directional constancy of the wind (defined as the ratio of vector to scalar mean wind speed) was particularly high during the winter of 1998, indicating a high degree of local

persistence to the northerly winds that were prevalent over the region.

[38] The impact of the decaying 1997/1998 ENSO on the sea ice and meteorological fields in the wAP area is evidently the root cause of the unusually deep, saline mixed layer created during winter 1998. However, there

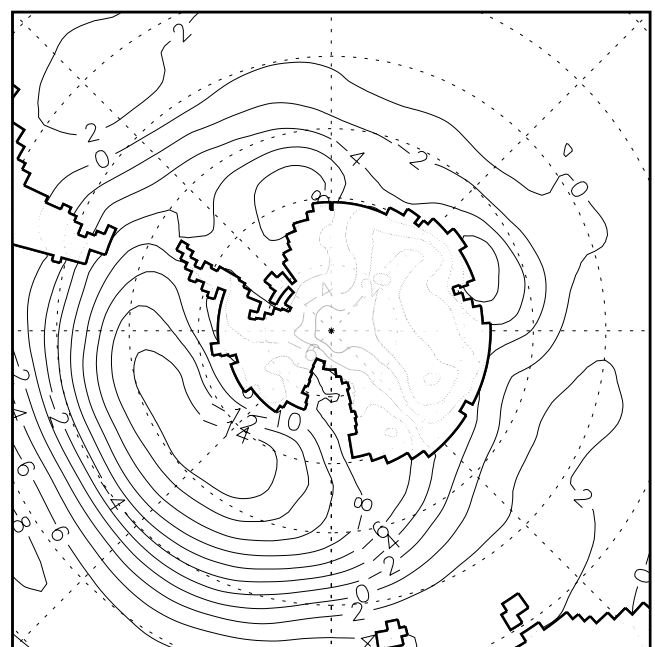


Figure 10. Mean sea level pressure anomaly (in hPa) for June–August 1998, relative to the 1971–2000 mean for this season. Data from the European Centre for Medium-Range Weather Forecasts 40-year reanalysis (ERA-40). The anomalous low pressure over the Amundsen-Bellinghousen Sea is associated with a greater frequency of northerly wind episodes at the western Antarctic Peninsula.

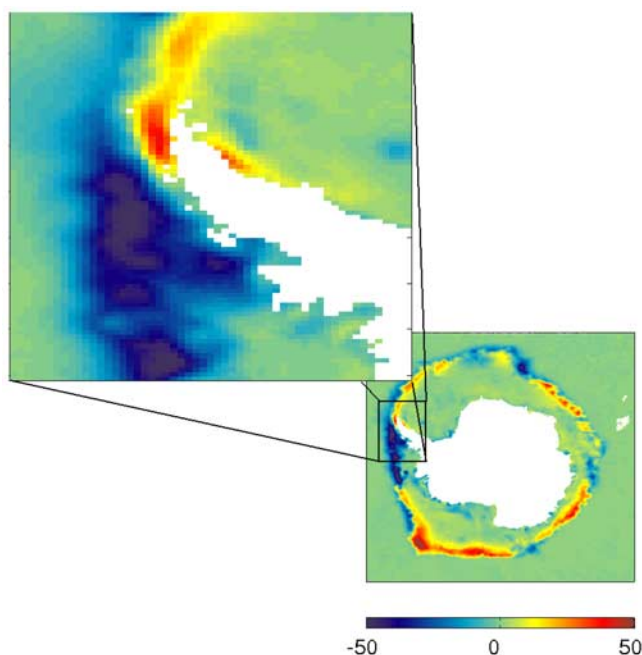


Figure 11. Sea ice concentration anomaly, August 1998 relative to long-term mean (1988–2001). Note the lower sea ice concentrations in the Bellingshausen Sea region, under the influence of the warmer northerly wind anomalies, and the extension of these low sea ice concentrations into northern Marguerite Bay (inset). Data are from the Special Sensor Microwave Imager (SSM/I).

are clearly a number of questions that need to be answered if we are to better understand its formation. Specifically, what processes caused the anomalous depth of the mixed layer, and hence the WW that it formed? One possible cause is enhanced salinification of the upper layers through greater brine rejection leading to denser water, and hence deeper seasonal convection; another is reduced sea ice coverage exposing the ocean to a higher air-sea momentum flux, thereby generating more near-surface mixing. Were the anomalous local air-sea fluxes and ice fields sufficient to explain the ocean anomalies, or was the broader ocean responding to larger-scale forcing, with advection also important? Addressing these questions prompts a related one: To what extent is our single-station time series representative of the larger-area WAP shelf?

[39] With such a paucity of direct oceanographic measurements from this area, any attempt to answer these questions using purely observational means is highly con-

strained. However, consideration of the meteorological forcings and the use of simple dynamical models that reliably represent some of the key processes can provide a great deal of information on these important questions.

4.3. Ice Production Model Results

[40] The derived monthly ice production totals (per unit area) over the study period, derived using the ice production model described in section 3.3, are shown in Figure 12. Ice is produced during May to November, with much month-to-month and interannual variability. *Renfrew et al.* [2002a] show that the month-to-month variability is often linked to synoptic-scale variability in the atmosphere, for example, the passage of low-pressure systems. Sea ice production in winter 1998 was 2.3 m over the year, a value that might seem initially rather high given the observation of persistently low sea ice concentrations for this area at the time (Figure 9). However, winter 1998 was characterized by persistent northerly winds (Table 1) that would have acted to drive ice southward out of Ryder Bay (which is closed to the north), maintaining a high open water fraction and high ice production rates. During 1999, the prevailing northerlies alternated with winds from other directions (reflected by the lower ratio of vector to scalar wind speeds in Table 1), allowing the development of a greater sea ice cover in Ryder Bay. However, estimated sea ice production for winter 1999 (1.8 m over the year) was not very much less than that in 1998 as the colder conditions during 1999 compensated for the lower open water fraction. The year 2001 showed the highest ice production during our sequence, totaling 3.0 m over the year, in excess of both 1998 and 1999. Yet 2001 was not particularly anomalous in the hydrographic record. We thus surmise that the relatively high local sea ice production in winter 1998 cannot be the sole cause of that year's anomalous ocean observations. The year of 2002 showed the lowest ice production during the 5-year period, a reflection of the near-total ice coverage from April to November acting to inhibit further ice formation at the surface, despite the extremely low air temperatures observed.

[41] Figure 13 shows the monthly mean wind stress exerted on the ocean as a function of time. It is derived as the time average of the stress magnitude from the meteorological observations at Rothera, using the surface-layer algorithms discussed earlier. The wind stress is weighted by the fraction of the surface not covered by fast ice (i.e., sea ice attached to land), thus accounting for the dynamical isolation of the ocean from the atmosphere by the ice. It can be seen that winter 1998 featured comparatively high effective wind stress, typically around 0.1 N m^{-2} on average, allowed by the relatively large amount of open

Table 1. Means for June, July, and August of Each Year for Selected Meteorological Data From Rothera

Year	Air Temperature, °C	Wind Speed, m s^{-1}	Vector-Mean Wind Speed, m s^{-1}	Vector-Mean Wind Direction	Vector/Scalar Wind Speed	Mean-Sea Level Pressure, mbar
1998	-5.11	7.75	5.20	20.3	0.67	981.9
1999	-7.90	6.79	1.17	2.2	0.17	991.5
2000	-7.29	6.52	3.40	0.0	0.52	995.1
2001	-8.72	6.97	3.06	3.6	0.44	987.0
2002	-13.76	5.85	2.81	7.0	0.48	994.1

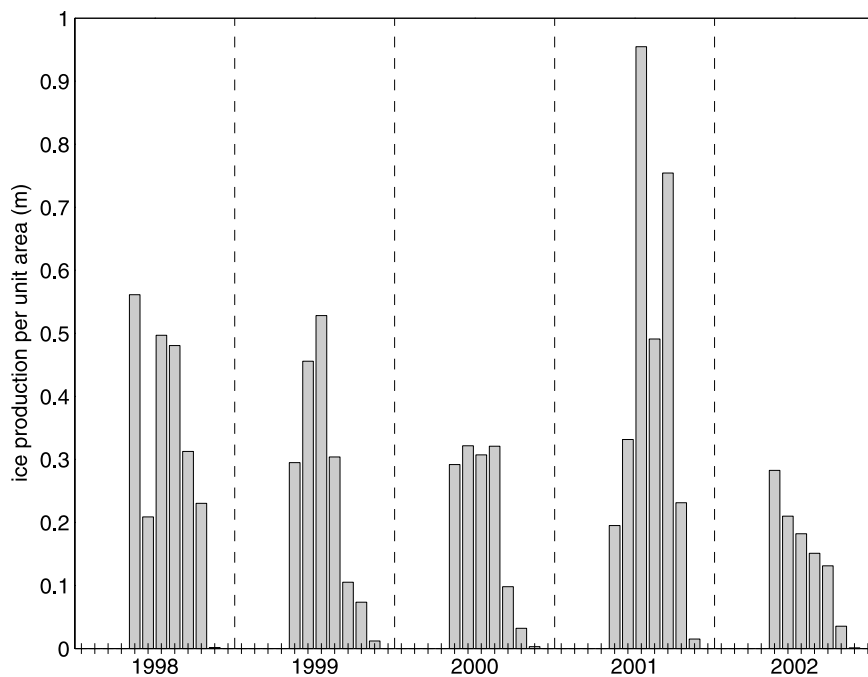


Figure 12. Accumulated ice production per unit area for each month, calculated using the sea ice production model described in the text. Note the high values in the austral winters of 1998 and 1999. Annual ice production totals are 2.3, 1.8, 1.4, 3.0, and 1.0 m for 1998 to 2002, respectively.

water (Figure 9). It should be noted, however, that winter 2001 also featured high effective wind stress, between 0.06 and 0.2 N m^{-2} in the winter, when the mixed layer was relatively shallow (Figures 3–5). Thus we surmise that the deep mixed layer seen in winter 1998 cannot be due solely to increased local wind-forced mixing.

[42] There are two remaining possibilities. The first is that the deeper mixed layer in 1998 could be the product of

both of the above phenomena, with increased salinity in the surface layer produced by local brine rejection acting to raise the density of the water, and the greater exposure of the ocean surface to the winds acting to induce mixing to greater depths. Such a combination of processes would be required, since neither process alone appears able to explain the depth of the mixed layer. The second possibility is that the anomalous oceanographic observations of

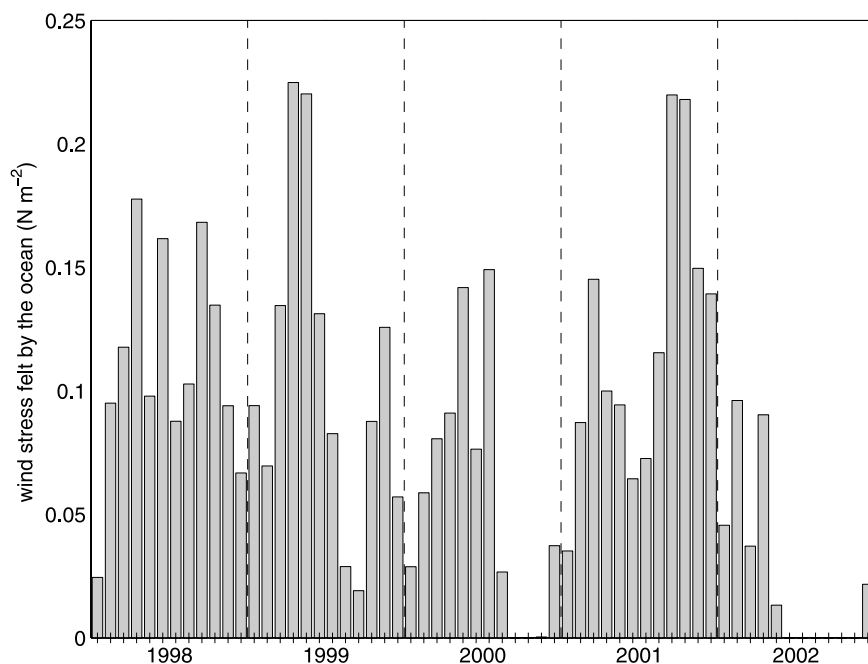


Figure 13. Monthly mean wind stress felt by the ocean, calculated by weighting by the area not covered by fast ice. Note the high monthly means during the austral winters of 1998 and 2001.

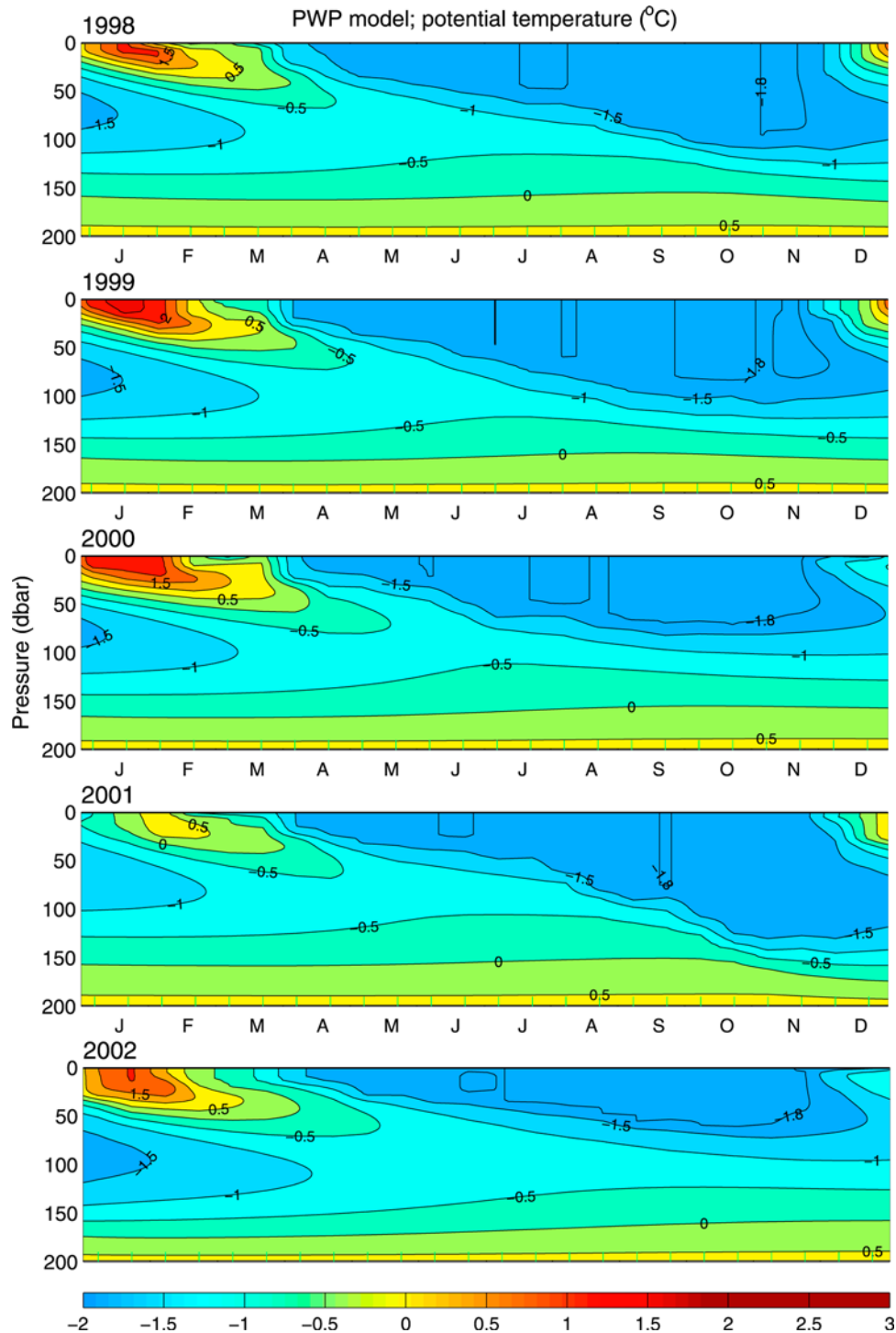


Figure 14. Simulated progression of potential temperature for the upper 200 m at the RaTS site (Ryder Bay, Figure 2), derived from the coupled ocean mixed-layer/ice production model (compare Figure 3). Output is contoured at 2-week intervals.

1998 might not have been the response to purely local fluxes and ice conditions. Rather, it could be that the large-scale meteorological and cryological forcings were dictating large-scale conditions over the wAP shelf, with oceanic advection involved in transferring these anomalies around the wAP area. In the absence of broad-area oceanographic data coverage from the wAP region in winter

1998, we resort to other means to assess these different possibilities.

4.4. Oceanographic Mixed-Layer Modeling

[43] Our oceanographic time series is from a single location, and there is not sufficient data from other places (especially wintertime data) to constrain a fully three-

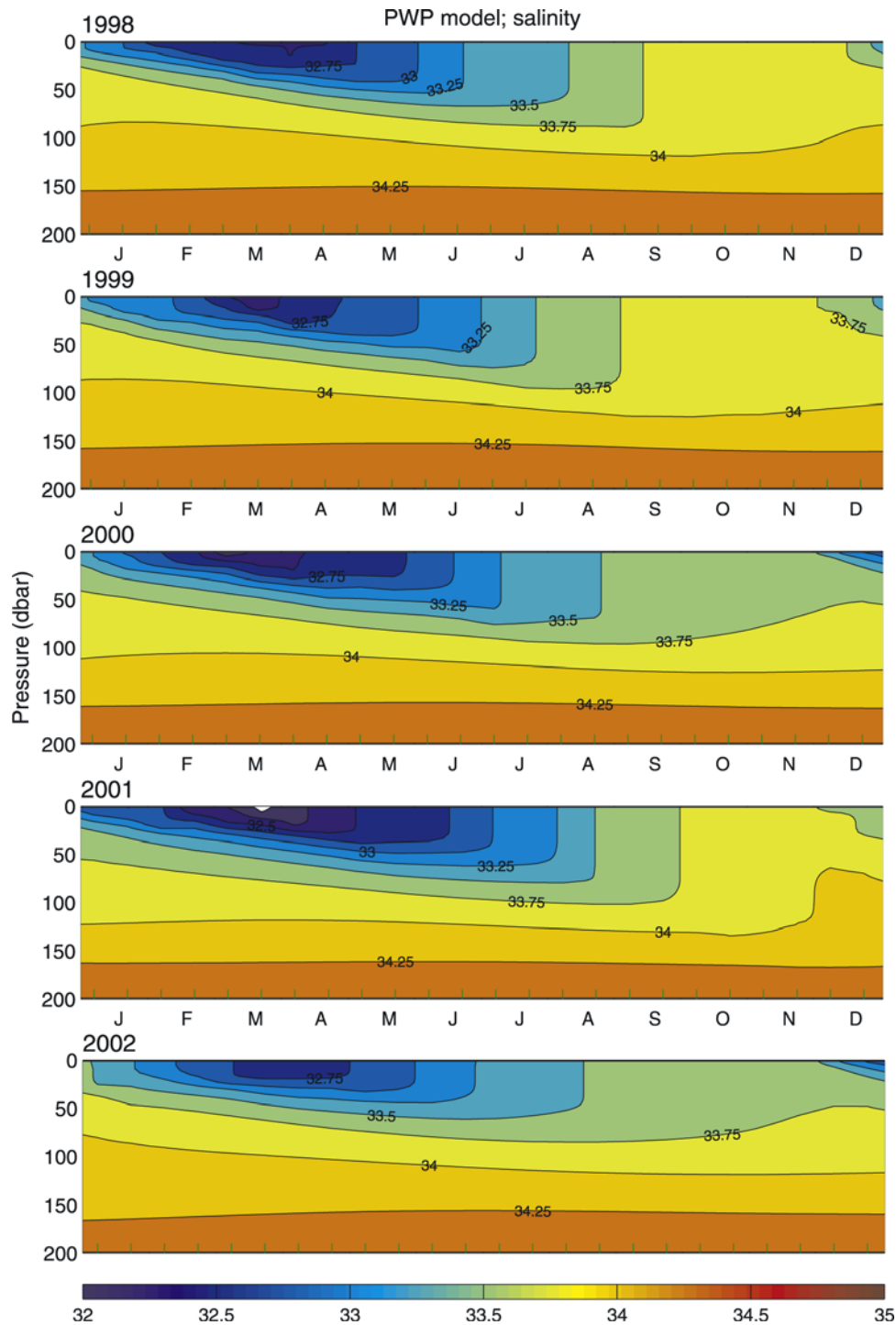


Figure 15. As for Figure 14, but for salinity (compare Figure 4).

dimensional model that would be suitable for addressing the issues under study. In particular, we lack good spatial coverage of air-sea flux measurements, ice production, and oceanographic data as validation. Instead, we constructed and ran an upper ocean mixed layer model based on that of PWP (see section 3.4), coupled to the sea ice production model summarized in section 3.3. Figure 14 shows the progression of potential temperature in the model for the period 1998–2002. There are strong similarities with the direct observations (Figure 3), as well as some differences.

[44] It is clear that the model captures the seasonal evolution of potential temperature. The warmest months in the model are January or February, with a deep winter mixed layer being created during May–July, seasonal stratification recommencing during December, and production of the temperature-minimum WW following the capping of the surface layers during the austral summer. The modeled temperature data appears smoother than the observations due to the absence of horizontal advection and mesoscale variability, i.e., its one-dimensional nature. This

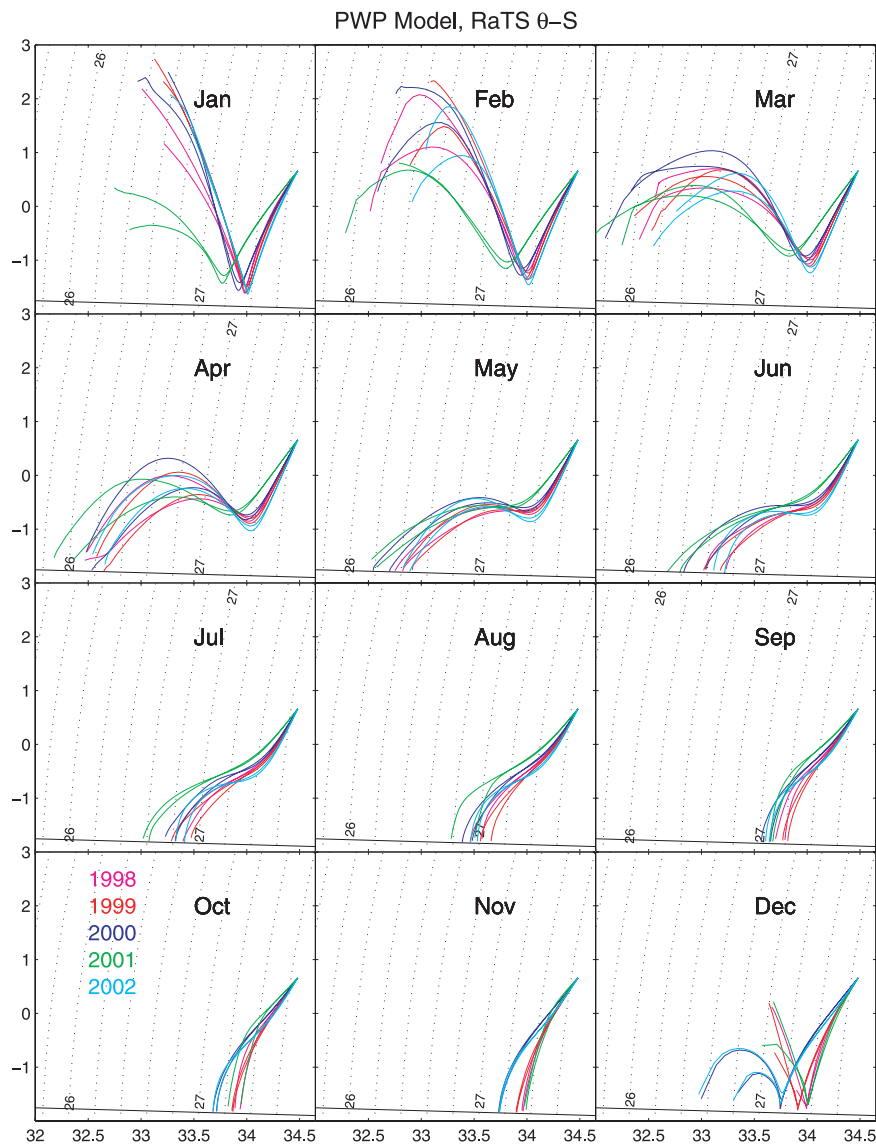


Figure 16. Simulated potential temperature-salinity properties for the RaTS sampling site (Ryder Bay, Figure 2), derived from the coupled ocean mixed-layer/ice production model (compare Figure 6). Panels are separate months (marked); curves are colored according to year: magenta (1998), red (1999), blue (2000), green (2001), and cyan (2002). Contours of density anomaly (σ_0) are plotted (dotted lines) at intervals of 0.2 kg/m^3 . The freezing line (solid line) is plotted across the base of each panel.

is most readily apparent in the deepest (UCDW) layer: Since the model treats this as a time-invariant water mass, any changes to this layer must derive via mixing from above. Of course, in the real ocean, variability in the intrusion of UCDW onto the shelf, and changes in its circulation, will induce variability in the UCDW properties at the sampling site, as seen in Figure 3. Nonetheless, it is clear that the model does a good job of reproducing the seasonal variability above the UCDW layer.

[45] The model salinity field (Figure 15) also agrees reasonably well with the measurements. The months with freshest surface waters are January/February through to April/May, following which the mixed layer becomes progressively deeper and more saline during the transition into winter. Again, the modeled salinity fields are smoother than the observations, and the UCDW layer is seen to be

much less variant, for reasons detailed above. Modeled density (not shown) strongly resembles modeled salinity, again due to the equation of state being dominated by salinity at low temperatures.

[46] The modeled water mass properties are shown in θ -S space in Figure 16. Seasonally, there is good agreement between these results and the oceanographic observations, although there are a few differences (for example, the model shows only a few hints of the near-isothermal layers that the observations revealed). January and February in particular show characteristic inflections, with minimum temperatures denoting the core of the WW. The invariance in the UCDW layer is seen as the θ -S curves converge completely in the model output. In a similar pattern to the observations, the curves show near-surface cooling during March and April, and by May the locus of surface water points are on the

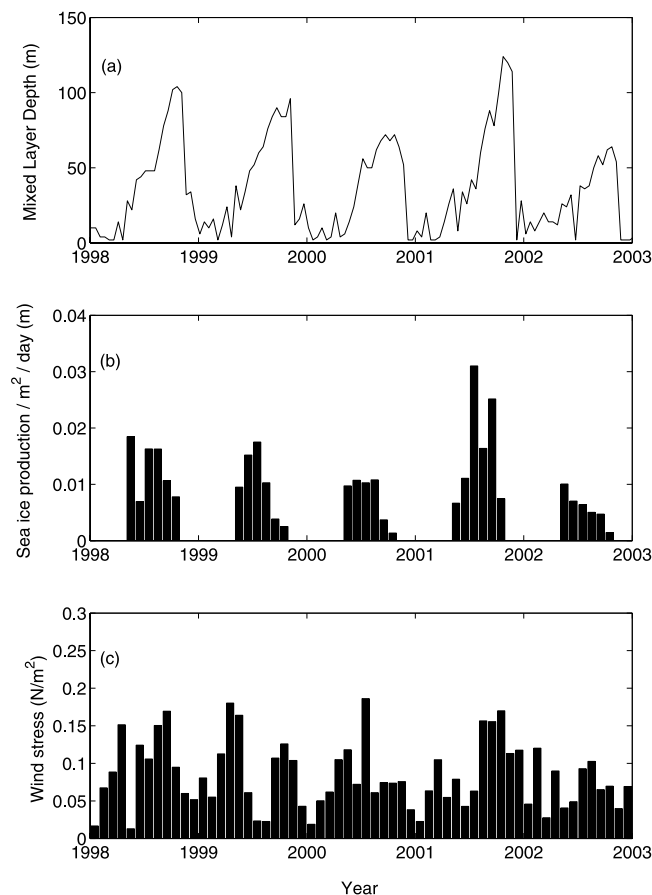


Figure 17. (a) Ocean mixed layer depth determined from the coupled mixed layer/ice production model. (b) Monthly mean sea ice production from the model (as per Figure 12). (c) Monthly mean wind stress. Note that years with stronger ice production induce a deeper mixed layer, while years with weaker ice production induce shallower mixed layers.

freezing line. During June to October, the curves become close to straight lines, and the salinity at the surface increases, peaking at around 34.0 in November. Seasonal warming and freshening recommences in December, with the temperature-minimum WW layer starting to be created.

[47] The good seasonal agreement between the observations and model output provides confidence that the model is capturing most of the important physical processes occurring on these timescales (with the possible exception of the UCDW variability). However, on interannual timescales, the model does a much poorer job at reproducing the observations. Most notably, the interannual variability in summer near-surface temperatures is different in the model compared with the observations, and the modeled winter mixed layer is not anomalously deep in winter 1998 compared with the other years. Note that the actual depth of the modeled mixed layer in winter is rather sensitive to the value of vertical diffusivity used; however, the interannual variability in its depth is robust.

[48] To gain a better understanding of the seasonal and interannual dynamical forcing of the upper ocean on the wAP shelf, we examined the model response to determine which forcings were predominant. Figure 17a shows the

oceanographic mixed layer depth (determined in the model as the depth to which the ocean is homogenized each time step), Figure 17b shows the monthly mean sea ice production (as derived for Figure 12 and used as one of the model's forcing variables), and Figure 17c shows the corresponding monthly mean wind stress. There is a clear relationship between the mixed layer depth and the ice production, with the mixed layer depth responding strongly during periods of strong ice formation (such as happens during 2001), and showing much less variance at other times. The mixed layer depth was shallowest in 2002, the year for which near-total ice coverage during April to November inhibited large sea ice formation, despite the very low air temperatures. The peak mixed layer depth for a given year clearly depends strongly on the integrated sea ice production during that year's winter. Comparison of wind stress with mixed layer depth revealed no such clear relationship. These results are in accord with *Smith and Klinck* [2002], who noted in their modeling study that winter mixed layers are deeper during years with high ice production.

5. Discussion and Summary

[49] The unusual, large-scale sea ice distribution in the austral winter of 1998, and similar such events in the past, have been widely noted to be consequences of ENSO [*Harangozo*, 2000; *Hanna*, 2001; *Meredith et al.*, 2003]. Here it has been observed that the decaying ENSO event of winter 1998 was associated with persistent northerly winds over the western Antarctic Peninsula, in addition to reduced sea ice concentrations. These unusual conditions were observed to coincide with anomalous upper ocean characteristics in northern Marguerite Bay, which showed very weak stratification that persisted into the following summer. Although there are two significant gaps in our upper ocean time series (austral winters of 2000 and 2001), it is still clear that the winter 1998 conditions were anomalous as the temperature-minimum WW formed at this time was by far the deepest and most saline of this period.

[50] While our oceanographic time series offers excellent temporal resolution, and (importantly) good wintertime coverage, a drawback is that data from a single location offer no insight into the spatial distribution of properties on the wAP shelf. To address the representativeness of the time series, a one-dimensional modeling approach has been used to test whether purely local forcing can explain the observed evolving properties of the water column. A coupled ice production/ocean mixed layer model offers significant insight into this: When locally forced, the model does a good job of reproducing the observed seasonal variability in oceanographic conditions, but does not reproduce the interannual variability. In particular, on the basis of forcing by local fluxes and ice production, the model was unable to replicate winter 1998 as a period with anomalous upper ocean conditions. The model forcings are based on simple physical models and are believed reliable, while the one-dimensional ocean dynamics have been used successfully in numerous other studies. Thus we surmise that key processes that are not included in the model must be important, most notably horizontal advection. We conclude that the anomalously deep, saline mixed layer observed during winter

1998, and the unusual WW that was created, are more likely associated with the unusual large-scale conditions that prevailed in the region of the wAP (e.g., Figure 11) than with the anomalous local forcing in northern Marguerite Bay. We have noted that the forcings for these changes are due to ENSO; accordingly, one can expect quasi-regular repeats of such conditions on interannual timescales. A fully three-dimensional regional model with realistic forcings and boundary conditions is desirable to investigate further the response of the waters on the wAP shelf to interannual variability in climatic forcing; this will, however, be difficult to validate given the spatial paucity of oceanographic observations from the region, particularly during winter. Data from the recent Southern Ocean GLOBEC cruises will be valuable in this context, but will not help with addressing the extremes observed in 1998.

[51] We have demonstrated that the upper ocean stratification in our study region is controlled strongly by ice production on interannual timescales. The influence of wind stress is less immediately obvious, though of course the winds do play a role in setting the ice conditions and determining ice production, and thus need to be included in any assessment. To the extent that the dynamics of our coupled mixed layer/ice production model are applicable over the broader wAP region (where the same water mass structure is generally present), however, it seems most likely that anomalous sea ice production caused the deep mixed layer in winter 1998, rather than anomalous directly wind-induced mixing. We have confidence that the model is realistically reproducing the ocean's response to local interannual forcing (i.e., the response the real ocean would have in the absence of advection, mesoscale variability, and larger-scale influences), since we observed that the mixed layer depth responds in a manner consistent with forcing by sea ice production. High levels of ice production (and consequent brine rejection) will have contributed to the greater salinity of the winter 1998 mixed layer, and the WW that it formed. In addition, the enhanced depth of the mixed layer will have led to greater excavation of the upper layer of the saline CDW; this will have entrained saline water upwards into the mixed layer, and further acted to raise the salinity there.

[52] It is important to note that the mixed layer model does not reproduce the observed variability in the UCDW structure throughout the 5-year period. This is not surprising: It would be most unlikely that variable air-sea fluxes and vertical mixing are predominant in controlling UCDW properties. Instead, variability in the input of UCDW to the wAP shelf and changes in its regional circulation are more likely to be important. We have recently commenced deeper CTD profiling (to nearly 400 m) and intend to introduce direct velocity measurements from fixed moorings into the suite of parameters being measured. These will better elucidate such processes, and help us to identify the effects of variability introduced into the upper layers by mixing from below.

[53] Understanding the causes of anomalously weak stratification has importance beyond the purely physical environment. Primary production in Antarctic waters is influenced strongly by variability in stratification, and phytoplankton blooms typically follow sea ice melt as stratification develops and light levels increase [McMinn,

1996; Clarke and Leakey, 1996]. Variability in the timing and intensity of summer blooms will thus be related to variability in sea ice dynamics, as well as in factors such as the input of UCDW onto the shelf [Prezelin et al., 2000]. Future work will focus on exploring this and related processes using the ongoing RaTS time series.

[54] In addition to interannual variability on ENSO timescales, the wAP has been subject to some of the most significant longer-term climatic changes observed in any region of the world in recent decades. The oceanographic impact of such changes are, as yet, almost completely unknown. This highlights that there is much to be learned about the response of the physical Antarctic marine environment to forcing on seasonal, interannual, and longer timescales. Other processes, such as increases in glacial ice melt and changes in precipitation, will also need consideration. Advanced three-dimensional coupled atmosphere-ocean modeling of the mixed layer and below will enable predictions to be made. However, the only way to test and improve the veracity of such models is to systematically monitor the Antarctic environment over long periods, and with sufficient temporal resolution to understand the relevant processes. The ongoing RaTS project will continue to contribute to this.

[55] **Acknowledgments.** We thank the many people at Rothera who braved the Antarctic elements to collect the data used here, in particular, Alice Chapman, Jenny Beaumont, Rayner Piper, Andy Miller, and the succession of Rothera boatmen. We are grateful to the scientists and crew of RRS *James Clark Ross* and RV *Laurence M Gould* for their support of this project, and to Bob Beardsley for providing the SO-GLOBEC bathymetric data. We are grateful to Gareth Marshall for extracting the ECWMF time series used here. We thank Laurie Padman and three anonymous reviewers, whose comments greatly improved the initial version of this paper. This project was funded by the Natural Environment Research Council.

References

- Ackley, S. F., C. Geiger, J. C. King, E. C. Hunke, and J. Comiso (1997), The Ronne polynya of 1997–98: Observations of air-ice-ocean interaction, *Ann. Glaciol.*, *33*, 425–429.
- Beardsley, R. C., R. Limeburner, and W. B. Owens (2004), Drifter measurements of surface currents near Marguerite Bay on the West Antarctic Peninsula Shelf during austral summer and fall, *Deep Sea Res., Part II, Southern Ocean GLOBEC Spec. Issue*, in press.
- Braithwaite, R. J. (1984), On glacier energy balance, ablation, and air temperature, *J. Glaciol.*, *27*, 381–391.
- Callahan, J. E. (1972), The structure and circulation of deep water in the Antarctic, *Deep Sea Res.*, *19*, 563–575.
- Clarke, A., and R. Leakey (1996), The seasonal cycle of phytoplankton, macronutrients and the microbial community in a nearshore Antarctic ecosystem, *Limnol. Oceanogr.*, *41*, 1281–1294.
- Cullather, R. I., D. H. Bromwich, and M. L. van Woert (1996), Interannual variations in Antarctic precipitation related to El Niño–Southern Oscillation, *J. Geophys. Res.*, *101*(D14), 19,109–19,118.
- DeCosmo, J., K. B. Katsaros, S. D. Smith, R. J. Anderson, W. A. Oost, K. Bumke, and H. Chadwick (1996), Air-sea exchange of water vapour and sensible heat: The Humidity Exchange Over the Sea (HEXOS) results, *J. Geophys. Res.*, *101*(C5), 12,001–12,016.
- Dierssen, H. M., R. C. Smith, and M. Vernet (2002), Glacial meltwater dynamics in coastal waters west of the Antarctic peninsula, *Proc. Natl. Acad. Sci. U.S.A.*, *99*(4), 1790–1795.
- Dinniman, M. S., and J. M. Klinck (2004), A model study of circulation and cross shelf exchange on the West Antarctic Peninsula continental shelf, *Deep Sea Res., Part II, Southern Ocean GLOBEC Spec. Issue*, in press.
- Hanna, E. (2001), Anomalous peak in Antarctic sea-ice area, winter 1998, coincident with ENSO, *Geophys. Res. Lett.*, *28*(8), 1595–1598.
- Harangozo, S. A. (1997), Atmospheric meridional circulation impacts on contrasting winter sea ice extent in two years in the Pacific sector of the Southern Ocean, *Tellus, Ser. A*, *49*, 388–400.
- Harangozo, S. A. (2000), A search for ENSO teleconnections in the West Antarctic Peninsula climate in austral winter, *Int. J. Climatol.*, *20*(6), 663–679.

- Hofmann, E. E., J. M. Klinck, C. M. Lascara, and D. A. Smith (1996), Water mass distribution and circulation west of the Antarctic Peninsula and including Bransfield Strait, in *Foundations for Ecological Research West of the Antarctic Peninsula*, *Antarct. Res. Ser.*, vol. 70, edited by R. M. Ross et al., pp. 61–80, AGU, Washington, D. C.
- Jacobs, G. A., and J. L. Mitchell (1996), Ocean circulation variations associated with the Antarctic Circumpolar Wave, *Geophys. Res. Lett.*, *23*(21), 2947–2950.
- King, J. C. (1994), Recent climate variability in the vicinity of the Antarctic Peninsula, *Int. J. Climatol.*, *14*, 357–369.
- King, J. C., and S. A. Harangozo (1998), Climate change in the western Antarctic Peninsula since 1945: Observations and possible causes, *Ann. Glaciol.*, *27*, 571–575.
- Klinck, J. M. (1998), Heat and salt changes on the continental shelf west of the Antarctic Peninsula between January 1993 and January 1994, *J. Geophys. Res.*, *103*(C4), 7617–7636.
- Klinck, J. M., E. E. Hofmann, R. C. Beardsley, B. Salihoglu, and S. Howard (2004), Water mass properties and circulation on the West Antarctic Peninsula continental shelf in austral fall and winter 2001, *Deep Sea Res., Part II, Southern Ocean GLOBEC Spec. Issue*, in press.
- Kwok, R., and J. C. Comiso (2002), Southern ocean climate and sea ice anomalies associated with the Southern Oscillation, *J. Clim.*, *15*, 487–501.
- McMinn, A. (1996), Preliminary investigation of the contribution of fast-ice algae to the spring phytoplankton bloom in Ellis Fjord, eastern Antarctica, *Polar Biol.*, *16*, 301–307.
- Meredith, M. P., C. W. Hughes, and P. R. Foden (2003), Downslope convection north of Elephant Island, Antarctic Peninsula: Influence on deep waters and dependence on ENSO, *Geophys. Res. Lett.*, *30*(9), 1462, doi:10.1029/2003GL017074.
- Meredith, M. P., E. J. Murphy, M. A. Brandon, P. N. Trathan, S. E. Thorpe, D. G. Bone, P. P. Chernyshkov, and V. A. Sushin (2004), Variability of hydrographic conditions to the east and northwest of South Georgia, 1996–2001, *J. Mar. Syst.*, in press.
- Mosby, H. (1934), The waters of the Atlantic Antarctic Ocean, *Sci. Result. Norw. Antarct. Exped. 1927–1928*, *11*, 1–131.
- Murphy, E. J., A. Clarke, C. Symon, and J. Priddle (1995), Temporal variation in Antarctic sea-ice: Analysis of a long-term fast-ice record from the South Orkney Islands, *Deep Sea Res.*, *42*, 1045–1062.
- Paulson, C. A., and J. J. Simpson (1977), Irradiance measurements in the upper ocean, *J. Phys. Oceanogr.*, *7*, 952–956.
- Peterson, R. G., and W. B. White (1998), Slow oceanic teleconnections linking the Antarctic Circumpolar Wave with the tropical El Niño–Southern Oscillation, *J. Geophys. Res.*, *103*(C11), 24,573–24,583.
- Prezelin, B. B., E. E. Hofmann, C. Mengelt, and J. M. Klinck (2000), The linkage between upper circumpolar deep water (UCDW) and phytoplankton assemblages on the West Antarctic Peninsula continental shelf, *J. Mar. Res.*, *58*, 129–136.
- Price, J. F., R. A. Weller, and R. Pinkel (1986), Diurnal cycling: Observations and models of the upper ocean response to diurnal heating, cooling and wind mixing, *J. Geophys. Res.*, *91*(C7), 8411–8427.
- Renfrew, I. A., J. C. King, and T. Markus (2002a), Coastal polynyas in the southern Weddell Sea: Variability of the surface energy budget, *J. Geophys. Res.*, *107*(C6), 3063, doi:10.1029/2000JC000720.
- Renfrew, I. A., G. W. K. Moore, P. S. Guest, and K. Bumke (2002b), A comparison of surface-layer and surface turbulent-flux observations over the Labrador Sea with ECMWF analyses and NCEP reanalyses, *J. Phys. Oceanogr.*, *32*, 383–400.
- Sievers, H. A., and W. D. Nowlin (1984), The stratification and water masses at Drake Passage, *J. Geophys. Res.*, *89*(C14), 10,489–10,514.
- Simpson, J. H. (1981), The shelf-sea fronts: Implications of their existence and behaviour, *Philos. Trans. R. Soc. London, Ser. A*, *302*, 531–546.
- Slingo, J. (1998), The 1997/98 El Niño, *Weather*, *53*, 274–281.
- Smith, D. A., and J. M. Klinck (2002), Water properties on the West Antarctic Peninsula continental shelf: A model study of effects of surface fluxes and sea ice, *Deep Sea Res., Part II*, *49*, 4863–4886.
- Smith, D. A., E. E. Hofmann, J. M. Klinck, and C. M. Lascara (1999), Hydrography and circulation of the West Antarctic Peninsula Continental Shelf, *Deep Sea Res., Part I*, *46*, 925–949.
- Smith, R. C., W. R. Fraser, S. E. Stammerjohn, and M. Vernet (2003), Palmer long-term ecological research on the Antarctic marine ecosystem, in *Antarctic Peninsula Climate Variability: A Historical and Palaeoenvironmental Perspective*, edited by E. Domack et al., pp. 131–144, AGU, Washington, D. C.
- Smith, S. D. (1988), Coefficients for sea surface wind stress, heat flux, and wind profiles as a function of wind speed and temperature, *J. Geophys. Res.*, *93*(C12), 15,467–15,472.
- U.N. Educational, Scientific, and Cultural Organization (1983), Algorithms for computation of fundamental properties of seawater, 1983, *Tech. Pap. Mar. Sci.*, *44*, 53 pp., Paris.
- Venegas, S. A., and M. R. Drinkwater (2001), Sea ice, atmosphere and upper ocean variability in the Weddell Sea, Antarctica, *J. Geophys. Res.*, *106*(C8), 16,747–16,765.
- Venegas, S. A., M. R. Drinkwater, and G. Shaffer (2001), Coupled oscillations in Antarctic sea ice and atmosphere in the South Pacific sector, *Geophys. Res. Lett.*, *28*(17), 3301–3304.
- White, W. B., and R. G. Peterson (1996), An Antarctic circumpolar wave in surface pressure, wind, temperature and sea-ice extent, *Nature*, *380*, 699–702.

M. A. Brandon, Department of Earth Sciences, Open University, Walton Hall, Milton Keynes MK7 6AA, UK. (m.a.brandon@open.ac.uk)

A. Clarke and J. C. King, British Antarctic Survey, High Cross, Madingley Road, Cambridge CB3 0ET, UK. (accl@bas.ac.uk; jcki@bas.ac.uk)

M. P. Meredith, Proudman Oceanographic Laboratory, Bidston Observatory, Prenton, Wirral CH43 7RA, UK. (mmm@pol.ac.uk)

I. A. Renfrew, School of Environmental Sciences, University of East Anglia, Norwich, NR4 7TJ, UK. (i.renfrew@uea.ac.uk)